separations

MDPI

Article

Assessing the Efficiency of Ion Exchange Resins for the Recovery of Scandium from Sulfuric Acid Leaching Solutions

Aikaterini Toli [1,*], Eleni Mikeli [1], Danai Marinos [1], Efthymios Balomenos [1,2] and Dimitrios Panias [1]

[1] School of Mining and Metallurgical Engineering, National Technical University of Athens, 15780 Athens, Greece; elenamikeli@mail.ntua.gr (E.M.); dmarinou@metal.ntua.gr (D.M.); efthymios.balomenos-external@alhellas.gr (E.B.); panias@metal.ntua.gr (D.P.)
[2] Mytilineos SA-Metallurgy Business Unit, Alumina and Aluminium Plant, 32100 St. Nikolas, Greece
* Correspondence: katerinatoli@metal.ntua.gr; Tel.: +30-2107722388

Abstract: Scandium, a valuable element with restricted production sources mainly situated in China and Russia, is typically obtained as a by-product during the production of various materials. As the demand for scandium grows in the expanding aluminum and fuel cell industries, and with significant investments in rare earth mining in the USA and Australia, there is a need to explore alternative recovery sources. This research investigates the recovery of scandium from an acid pregnant leaching solution using ion exchange resins. The pregnant leaching solution was obtained after the leaching of bauxite residue with sulfuric acid. Commercial resins with different functional groups were tested for their performance in scandium extraction. In addition, the co-adsorption of impurities, such as iron and titanium, was studied. The feed solution consisted of 12.7 mg/L Sc and main impurities of 272 mg/L Fe and 33.6 mg/L Ti and was pretreated before the ion exchange process by acidification with sulfuric acid and iron powder addition to suppress silica gel formation and minimize the Fe(III) content in the solution accordingly. Among the tested resins, a D_2EHPA-impregnated resin had high selectivity for Sc towards Ti, while a monophosphonic resin was also a promising option since it had a higher capacity for Sc but co-extracted Ti. These findings offer promising opportunities for the recovery of scandium from acid leaching solutions and could contribute to addressing the growing demand for this valuable element.

Keywords: D_2EHPA-impregnated resin; monophosphonic resin; sulfuric acid; leaching; scandium; adsorption isotherms; ion exchange

Citation: Toli, A.; Mikeli, E.; Marinos, D.; Balomenos, E.; Panias, D. Assessing the Efficiency of Ion Exchange Resins for the Recovery of Scandium from Sulfuric Acid Leaching Solutions. *Separations* **2023**, *10*, 366. https://doi.org/10.3390/separations10070366

Academic Editor: Chunjian Zhao

Received: 10 May 2023
Revised: 12 June 2023
Accepted: 19 June 2023
Published: 21 June 2023

1. Introduction

Scandium (Sc) is a rare earth element with unique properties that make it highly valuable for a variety of industrial applications, including aerospace, electronics, and renewable energy [1,2]. According to the EU, it is also a critical raw material (CRM) due to its high supply risk and economic importance [3–6]. The current production of scandium has been insufficient to meet the anticipated increase in demand by 2028, despite its critical role in various technologies, such as solid oxide fuel cells (SOFCs) and lightweight aluminum alloys [6]. Although the global consumption of scandium is presently below 300 tons annually, its supply remains a significant concern [7]. In addition, while Sc is relatively abundant in the earth's crust, it is found in trace amounts in various ores, and during industrial processing, it is commonly accumulated in the waste streams. China and Russia are the primary global producers of scandium, with China currently holding the dominant position in the market [8]. China's production of scandium primarily relies on the extraction of this element as a by-product during the processing of various rare earth minerals, bauxite residue, as well as specific titanium and zirconium ores [9,10]. Russia possesses significant reserves of scandium, particularly in the form of scandium-enriched ores [11]. Similar to China, Russia also explores rare earth deposits, such as magnetite, iron,

and uranium deposits that contain scandium and extracts it as a by-product during the processing of these deposits for rare earth elements [9,11]. Nevertheless, both dominating countries, in terms of scandium production, encounter several limitations associated with the variable scandium content in deposits, complex extraction processes, production costs, and infrastructure challenges [12]. Many researchers have investigated the possibility of recovering secondarily Sc from the by-products and waste streams of the iron, uranium, titanium, and aluminum industries [8,13–19] Bauxite residue, also known as red mud, which is the main by-product of the alumina-refining process, typically contains small amounts of scandium (up to 100 mg/kg), which is considered sufficient for scandium valorization [8,20].

The worldwide accumulation of bauxite residue (BR) disposed of in landfills is more than 2.7 billion tons, and it is currently increasing at an annual rate of over 120 million tons [21]. About 1–2 metric tons of bauxite residue is generated for each ton of alumina produced [22]. The production of bauxite residue poses a significant environmental concern due to its alkaline nature and the need for its storage in holding facilities. The high pH of the residue can lead to soil and water contamination, while the storage of large quantities of red mud requires extensive land use and is uneconomic [23–26]. Greek BR is especially chemically stable and contains various metals, including a significant amount of Sc (up to 120 mg/kg), making it a promising resource for Sc extraction [27,28]. Davris et al., 2022, developed research under the H2020-SCALE project, which aimed at an industrial operation for scandium extraction from Greek BR through a hydrometallurgical process [29]. Within this project, sulfuric acid was chosen as the best leaching agent based on its scandium extraction selectivity, low cost, and ease of handling. However, the recovery of scandium from such solutions is challenging due to the considerably low concentration of scandium (~12 mg/L) compared to the numerous impurities, present in higher concentrations, such as iron (~300 mg/L) and titanium (~30 mg/L) [29].

Ion exchange processes have proven to be effective at recovering and purifying a variety of metals on an industrial scale, and in recent years, they have emerged as a promising technology for the recovery of scandium from acid leaching solutions [16,30–33]. The most used resins for scandium recovery are strong acidic cation exchange resins, such as sulfonic acid or carboxylic acid resins [34,35]. Recently, impregnated resins have been gaining popularity as an effective method for scandium recovery, with liquid neutral organophosphorus and alkyl phosphoric acid compounds being commonly employed as extractants [32,36,37]. Mostajeran et al., 2021, studied a series of ion exchange resins for the recovery of Sc from synthetic and actual pregnant leach solutions obtained from the acid leaching of coal fly ash [38]. Sc was adsorbed quickly on phosphorus containing Lewatit VPOC 1026 and TP 272 resins even in the presence of high levels of potentially interfering Fe^{3+} and Al^{3+} ions. Altinsel et al., 2018, investigated the extraction of scandium from laterite ore using different resins. Amberlite IRC 747 and Lewatit TP 260 resins have loaded scandium perfectly. Both Amberlite IR 120 and Amberlite 402 resins did not show consistent loading tendencies for scandium. The operating capacities of Amberlite IRC 747 and Lewatit TP 260 for scandium were determined as 5 and 6 g Sc/L of resin, respectively [39].

This study investigated the potential of ion exchange resins for the recovery of scandium from acid pregnant leaching solutions (PLS) obtained from the leaching of bauxite residue with sulfuric acid. More specifically, resins with different properties were studied for the adsorption of scandium. The experiments were conducted in batches following a standard protocol for the adsorption of scandium. The study aimed to identify the most promising adsorbents to selectively recover scandium from sulfuric acid leaching solutions obtained from BR.

2. Materials and Methods

In this study, nine different cation exchange resins were evaluated for their scandium adsorption behavior from a sulfuric acid leachate solution. Initially, screening loading

experiments were conducted to determine the best-performing resin(s) in terms of their scandium adsorption capacity from a standard feed solution. The best-performing resins were also evaluated for their selectivity in scandium extraction towards iron and titanium. The effect of the pH and iron ion valence of the feed solution was also investigated in terms of its scandium adsorption and selectivity for different metals. In the optimum adsorption conditions, kinetic experiments were also conducted.

2.1. Materials

The cation exchange resins used in this study and their characteristics are outlined in Table 1. These resins share a polystyrene crosslinked matrix structure but differ in their functional groups, which are also listed in Table 1. Among the resins selected for this study, many contain phosphorus-based functional groups, which are known to form strong complexes with Sc, such as aminomethyl-phosphoric acid (IRC 747, TP 260, CH 93), monophosphoric acid (LSC 730), di-ethylhexyl phosphoric acid, D_2EHPA (LSC 790), and bis (2,4,4-trimethylpentyl) phosphinic acid (TP 272). The other resins selected contained iminodiacetic acid, IMA (TP 208, TP 209), and sulfonic acid (IRC 120). All the resins received in the sodium form were conditioned with 1.5M HCl acid prior to the ion exchange experiments to ensure that they were completely converted into the hydrogen form according to their available datasheets. For the resins received in the hydrogen form, no conditioning step was applied.

Table 1. Resins with different functional groups and their properties obtained from datasheet specifications available for each resin.

	Properties			
Resins	**Functional Group**	**Capacity (eq/L)**	**Form Received**	**Operating pH**
Seplite LSC 730	Monophosphonic	18 g/L (Fe)	H+	(NA)
Seplite LSC 790	D_2EHPA impregnated	(NA)	H+	<4
Lewatit TP 260	Aminomethyl phosphonic acid	2.4 min. eq/L	Na+	0–14
Amberlite IRC 747	Amino phosphonic	1.75 eq/L	Na+	(DA)
Amberlite IRC 120	Sulfonic acid	1.8	H+	0–14 (S)
Lewatit TP 209	Iminiodiacetic acid	2.4 min. eq/L	Na+	2–10
Lewatit TP 272	Bis-(2,4,4-trimethylpentyl) phosphinic acid	12.5 g/l (Zn) min eq/L	H+	1–6
Tulsion CH-93	Aminomethyl phosphoric	2 min. eq/l	Na+	0–14 (S)
Lewatit TP 208	Iminiodiacetic acid	2.9 min. eq/L	Na+	2–12

NA: Not available, DA: depends on the application, S: stable.

All chemical reagents were of analytical reagent grade. Fine iron powder and sulfuric acid solution were purchased from Sigma Aldrich, St. Louis, MO, USA.

The acid pregnant leaching solution (PLS) that was used in this work was obtained from the sulfuric acid leaching of bauxite residue, which was produced in a pilot plant at MYTILINEOS S.A., Agios Nikolaos, Greece. Table 2 shows the composition of the PLS.

2.2. Characterization of Liquid Samples

The chemical composition (Fe, Sc, Ti) of liquid samples obtained during the course of this work was determined with ICP-OES using an Optima 7000, Perkin Elmer, Akron, OH, USA. The stable oxidation state of scandium in an aqueous solution is Sc(III), and of titanium, Ti (IV) [40,41]. The pH measurements were carried out with a pH meter Metrohm 913 laboratory version equipped with a Unitrode 3 m KCl pH electrode, Metrohm AG, Herisau, Switzerland. The Fe (II) was determined colorimetrically with 1,10-phenanthroline at 510 nm, using a UV-Visible spectrophotometer Hitachi (U1100). For the batch adsorption experiments, an orbital incubator was used to agitate the adsorbate–adsorbent mixtures.

Table 2. Composition and pH of the initial feed solution obtained from the leaching of bauxite residue with H_2SO_4 solution.

Initial Solution	
pH	3.6
Composition (mg/L)	
Al	8000
Ti	33.6
Ca	562.9
Sc	12.7
Si	93.7
Ga	2.5
Na	14,600
K	133.7
SO_4^{2-}	78,100
Fe total	272
Fe (II)	172.3
Fe (II)%	63.3

2.3. Preparation of Feed Solution

The feed solution used in this study was obtained from pilot-scale leaching experiments of bauxite residue with sulfuric acid (Table 2). Based on previous studies [37], the obtained leachate solution (PLS) had a pH of 3.6 and was supersaturated at an ambient temperature, and therefore, amorphous aluminum silicate slowly precipitated out of the solution. Furthermore, the PLS had a relatively higher content of total iron compared to scandium. More specifically, Fe (III), which is known to act competitively to Sc (III) during ion exchange, made up 36.9% of the total iron of the PLS (Table 2) [42]. Therefore, to make the solution undersaturated and to minimize the Fe (III) content, the feed solution underwent a pretreatment step prior to the ion exchange procedure.

Particularly, the PLS was filtrated, the pH was subsequently adjusted by acidification with sulfuric acid, and the Fe (III) was reduced to Fe (II) with the addition of metallic iron powder. The pretreatment of the solution was conducted using an orbital shaker for 24 h at 220 rpm at room temperature. The undissolved metallic iron powder was then separated with vacuum filtration.

The initial screening of the different ion exchange resins was performed with a standard treated solution prepared with the addition of 0.3 g of iron powder and 17 mL of concentrated H_2SO_4 (18M) per liter of PLS [37]. The changes in the final treated PLS in terms of Fe and pH are shown in Table 3.

Table 3. Composition of iron in the final treated solution.

	Fe Tot. (mg/L)	**Fe (II) (mg/L)**	**Fe (II) %**	**pH**
Treated solution	587.3	559.9	95.34	0.7

The most promising resins for Sc extraction were evaluated under different pretreated feed solutions.

2.4. Batch Adsorption Studies

2.4.1. Experimental Procedure

The capacity of the resins to adsorb Sc from a sulfuric acid leaching solution was evaluated through batch equilibrium experiments. In these experiments, an amount of resin of known weight was added to glass Erlenmeyer flasks with a known volume of the pretreated solution with various ratios to the resin mass, ranging from 50:1 to 1200:1 mL solution/g resin. The flasks were plugged with a glass stopper and shaken in an incubator shaker at a fixed rotation speed of 220 rpm, ambient temperature, and retention time of 24 h.

After completion of the batch experiment, the resin and solution were separated through vacuum filtration, and the solution was prepared for chemical analysis.

The kinetics of adsorption were studied for the best-performing resins in three different ratios of the solution volume (ml) to the mass of resin (g): 250:1, 500:1, and 1000:1. The kinetic experiments were carried out in an incubator at ambient temperature and 50 rpm, and samples of the supernatant solution were collected at various time intervals, including 10, 20, and 30 min, 1, 2, 4, and 8 h, and 1 to 3 days for analysis.

Equation (1) was used for the determination of the metal quantity adsorbed, where *qt* is the capacity of the resin at equilibrium in the mass of metal ion adsorbed per mass of resin (mg/g), C_0 and C_t are the metal concentrations (mg L^{-1}), V is the volume of the solution (L), and m is the mass of the resin (g) on a dry basis. Equation (2) was used to quantify the percentage of metal adsorbed by the resins.

$$q_t = (C_0 - C_t)\frac{V}{m} \tag{1}$$

$$\%A = \frac{(C_0 - C_t)}{C_0}100\% \tag{2}$$

2.4.2. Adsorption Isotherm Studies

The effectiveness of metal adsorption by the resins was studied through the adsorption isotherms. Two different adsorption models were studied, the Freundlich (Equation (3)) and Langmuir (Equation (4)) ones [36].

$$q_e = K_F C_e^{1/n} \tag{3}$$

where *Ce* (mg/L) is the equilibrium concentration of metal in the aqueous phase, *qe* (mg/g) is the equilibrium concentration of metal in the resin, and K_F ($mg^{(1-1/n)}$ g^{-1} $L^{1/n}$) and $1/n$ are the parameters of Freundlich's isotherm.

$$q_e = \frac{q_m K_L C_e}{1 + K_L C_e} \tag{4}$$

where *qm* (mg/g) is the maximum adsorption capacity, and K_L (L/mg) is the Langmuir isotherm constant.

2.4.3. Adsorption Kinetic Studies

Pseudo-first-order and second-order kinetic models were used to describe the experimental data, using Equations (5) and (6), respectively [43].

$$\begin{array}{c} \frac{d_q}{d_t} = k_1(q_e - q) \\ \ln(q_e - q_t) = lnq_e - k_1 t \end{array} \tag{5}$$

where q_t (mg/g) is the concentration of metal on the resin at time t, and k_1 (min $^{-1}$) is the pseudo-first-order kinetic constant.

$$\begin{array}{c} \frac{d_q}{d_t} = k_2(q_e - q)^2 \\ \frac{t}{q_t} = \frac{1}{k_2 {q_e}^2} + \frac{1}{q_e} \end{array} \tag{6}$$

where k_2 (mg g^{-1} min^{-1}) is the pseudo-second-order kinetic constant.

3. Results and Discussion

3.1. Screening of Different Resins

The Sc adsorption on the resins studied for several solution-to-resin ratios is shown in Figure 1.

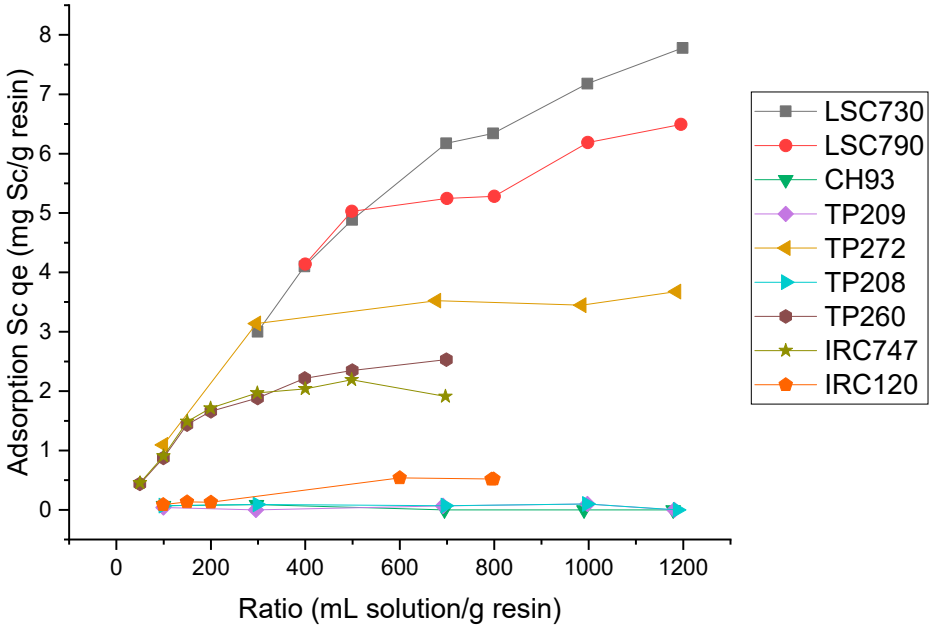

Figure 1. Scandium adsorption capacity (mg Sc/g resin), of different commercial resins at different ratios of solution/resin, amb. temperature, 220 rpm, 24 h.

According to the results, TP 208, TP 209, and CH-93, with iminiodiacetic acid and aminomethylphosphoric functional groups, had a near-zero adsorption capacity, while IRC 120, IRC 747, TP 260, and TP 272, with sulfonic, aminophosphonic, aminomethyl phosphonic acid, and bis-(2,4,4-trimethylpentyl-) phosphinic acid functional groups, respectively, exhibited a maximum capacity from 2 to 3 mg Sc/g resin [38,42,44].

A comparison to other studies can be seen in Table 4, providing a comprehensive overview of the primary investigations conducted on the adsorption of scandium using various resin materials. The table outlines the parameters explored in these studies and presents the key findings obtained.

Alexey et al., 2017, studied scandium and thorium sorption from uranium leach liquors by phosphorous-containing ion exchange resins. The findings of their study align with the results obtained in this study, which suggest that the exchange capacity of Tulsion CH-93 was low, at 0.28 mg of Sc/g resin [44]. Another study by Bao et al., 2018, focused on scandium loading on chelating and solvent-impregnated resin from a sulfate solution in a liquid-to-solid (L/S) ratio equal to 1 and a pH of solution equal to 2.5. The results indicate that the adsorption rates of Sc in 24 h were 58%, 15%, and 9% for the TayP 260, TP 209, and TP 272 resins, respectively [42]. Moreover, Mostajeran et al., 2021, studied scandium and rare earth elements' selective recovery from coal fly ash leach solutions. They used an L/S ratio equal to 100:1, with a 48 h retention time and a pH equal to 1.6. The results of their study showed that almost no scandium was loaded on resins TP 208 and TP209, while TP 260 and TP 272 experienced high adsorptions of 38% and 76%, respectively [38]. Seplite LSC 790 resin, which is D_2EHPA-impregnated, performed a high adsorption capacity of 6.49 mg Sc/g resin at an L/S ratio of 1200:1 and LSC 730, with the monophosponic functional group presenting the highest adsorption capacity of Sc up to 7.78 mg Sc/g resin at the same L/S ratio. Additionally, the same group studied a D_2EHPA-impregnated resin (Lewatit®VP OC 1026, Lenntech, Delfgauw, The Netherlands), which exhibited over a 99% adsorption of Sc, thereby highlighting the critical role of phosphorus groups in the recovery of Sc by IX resins. With a high concentration of ferric ions in the solution, the iminodiacetate sites in TP 208 and TP 209 could be saturated very quickly with Fe, preventing these resins from adsorbing Sc. The results of the present study are consistent with these findings, which suggest that the D_2EHPA-impregnated resin performs better in adsorbing scandium.

Table 4. Sorption of scandium from different ion exchange resins.

Sorbent	Parameters Studied	Composition of Solution	Sc Sorption Capacity	Ref.
Activated carbon (AC), carbon nanotubes (CNTs), graphene oxide (GO), and chelating resin Chelex 100	pH range: 1–5.5 Sc(III) concentration range: 1–300 mg/L	Synthetic Sc (III) solution	At pH 2, 2.1, 2.9, 36.5, and 37.9 mg of Sc/g of resin capacity was obtained for AC-COOH, Chelex 100, GO, and CNTs COOH, respectively. At pH 4, a similar value was obtained for oxidized AC (2.2 mg g^{-1}), whereas the specific amount adsorbed significantly increased for Chelex (23.4 mg g^{-1}). The highest values were obtained for GO (39.7 mg/g) and oxidized CNTs (42.5 mg g^{-1}).	[45]
Purolite MTS9580 and Lewatit TP260	Mother liquor solution, pre-acidified H_2SO_4: 5, 10, 15 g/L pH =2	Sc 0.34 mg/L, U 1.9 mg/L, Ce 3.82 mg/L, Nb 6.25 mg/L, Y 1.66 mg/L, Fe^{2+} 40 mg/L, Fe^{3+} 140 mg/L, Al 160 mg/L, Th 0.084 mg/L	Comparison of scandium sorption from pre-acidified uranium sorption mother liquor with Lewatit TP260 and Purolite MTS9580 ion exchangers showed an advantage for MTS9580 resin. The MTS9580 resin had an exchange capacity of 200 mg Sc/L of resin versus 59.7 mg Sc/L of resin for TP260.	[46]
Amberlite XAD-4 resin, impregnated with di(2-ethylhexyl) phosphoric acid (D2EHPA)	Adsorbent dosage (0.1–3.0 g), time (10 min to 24 h), pH = 2–9, initial Sc concentration (0.5–4 mg/L)	10 mg dm^{-3} scandium stock solution	A maximum capacity of 0.035 mg Sc3+/g of resin was achieved.	[47]
Purolite RUA21207 ion exchange resin	Different concentrations (25–200 g L^{-1}) of sulfuric acid solutions	Scandium concentrate (0.022 g/L) generated from acid waste of titanium white production has been dissolved in 25 g/L H_2SO_4	Sorption was favored at 25 g L^{-1} H_2SO_4 in solution when the initial scandium concentration was 6.4 mg/g.	[48]
Lewatit TP 260, TP 272, TP 208, TP 209, SP 112, VP OC 1026 resins	Several synthetic PLSs and several resins	PLS with Ce (3.2 mg/L), Dy (0.6 mg/L), La (1.3 mg/L), Nd (1.7 mg/L), Sc (1.1 mg/L), and Y (4.0 mg/L). The stock solution with Sc equal to 1250 mg/L in 0.5 M H_2SO_4	Sc was adsorbed on phosphorus containing Lewatit® VP OC 1026 and TP 272 resins, with a maximum capacity of ~24 mg Sc/g resin, even in the presence of high levels of potentially interfering Fe^{3+} and Al^{3+} ions.	[38]
Purolite D 5041, Tulsion CH 93, Lewatit TP 260, Purolite S 950 resins	Sorption recovery under dynamic conditions; the solution was passed through a 5 mL column at a flow rate of 25 mL/h	The sulfuric acid concentration in the uranium leach liquor was 5 g/L. Sc (0.78 mg/L), Th (1.81 mg/L), Al (2086.5 mg/L), Fe (1488.8 mg/L), Ti (2.47 mg/L), U (0.92 mg/L).	An increase in thorium concentration resulted in a decrease in scandium sorption by 26–65%. Tulsion CH 93 resin was chosen for Sc separation from uranium leach liquors.	[44]
Lewatit TP260 and TP 209 resins, and one solvent impregnated resin with bis(2,4,4-trimethylpentyl) phosphinic acid (TP 272)	Contact time (0–50 h) pH (1–3) Different sulfate concentrations (0, 0.25, 0.5, 1, and 1.5 M) Temperature (20–80 °C)	Synthetic sulfate leach solutions with 50 mg Sc/L	The adsorption capacity of TP 260 and TP 209 for Sc increased with pH from 1 to 3. TP 209 did not adsorb Sc at pH 1 but the adsorption capacity of TP 260 reached 35.5 mg Sc/g-dry at pH 1 and Sc also adsorbed onto TP272 at pH 1.	[42]

Consequently, the resins, namely LSC 730 and LSC 790, with a superior adsorption capacity, were chosen for further investigation in the present study.

3.1.1. Investigation of Iron and Titanium Adsorption by Batch Experiments

The two resins that had the higher performance in scandium adsorption were selected for further investigation and evaluated for their performance in scandium, iron, and titanium adsorption with different solution-to-resin ratios. The experiments were conducted in duplicate to ensure replicability and to enhance the reliability of the results. The results are presented in Figure 2.

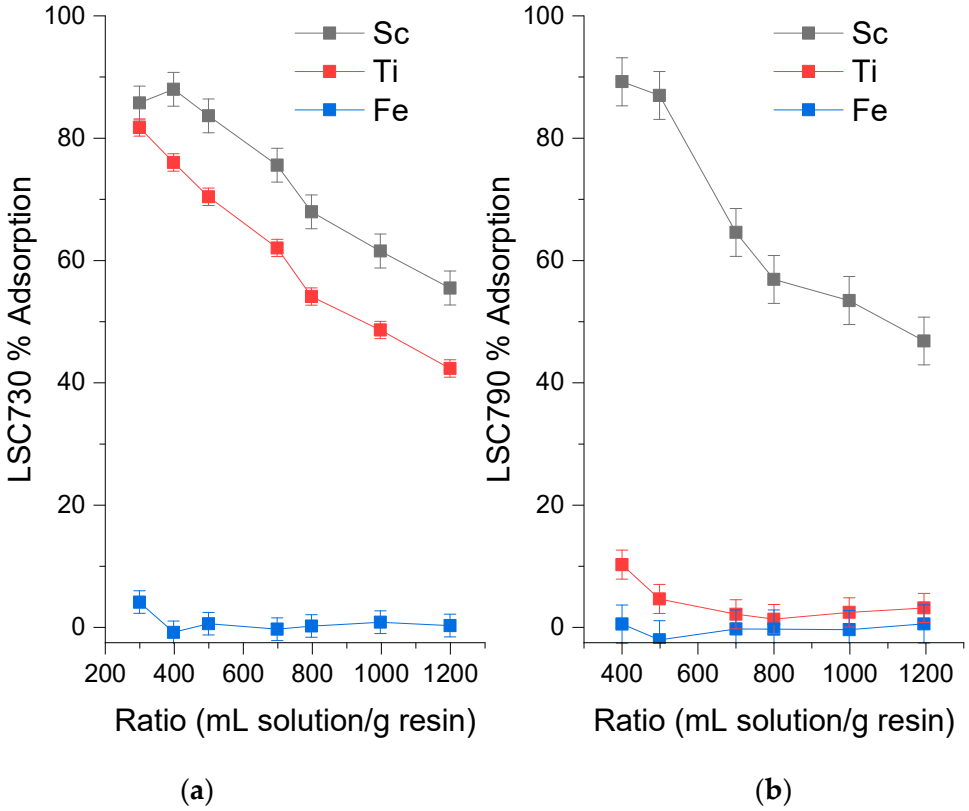

Figure 2. Adsorption rates of Sc, Ti, and Fe from feed solution at different ratios of solution/resin, amb. temperature, 220 rpm, 24 h using (**a**) LSC 730 resin and (**b**) LSC 790 resin.

Figure 2a demonstrates the simultaneous adsorption of Sc and Ti up to 85.75% and 82.7% at a ratio of 300:1, respectively, for the resin LSC 730, while the adsorption of Fe was insignificant, with a maximum adsorption of 4%. On the other hand, LSC 790, shown in Figure 2b, performed maximum adsorptions of 89.22% Sc, 10% Ti, and 0.5% Fe, at a 300:1 ratio.

3.1.2. Adsorption Isotherms

The adsorption isotherms of Sc into the two resins are presented in Figure 3. The results were analyzed by fitting the experimental data to the Freundlich and Langmuir models. Table 5 displays the correlation coefficients between the experimental and calculated values, as well as the parameters of the Freundlich and Langmuir models. As reported earlier, the adsorption of Fe was found to be 4% for the LSC 730 resin, whereas, for LSC 790, the adsorption percentages of Ti and Fe were 10% and 0.5%, respectively (refer to Figure 2a,b). Therefore, while fitting the Freundlich and Langmuir models to the experimental data, only scandium and titanium were considered for LSC 730, and only scandium was considered for LSC 790.

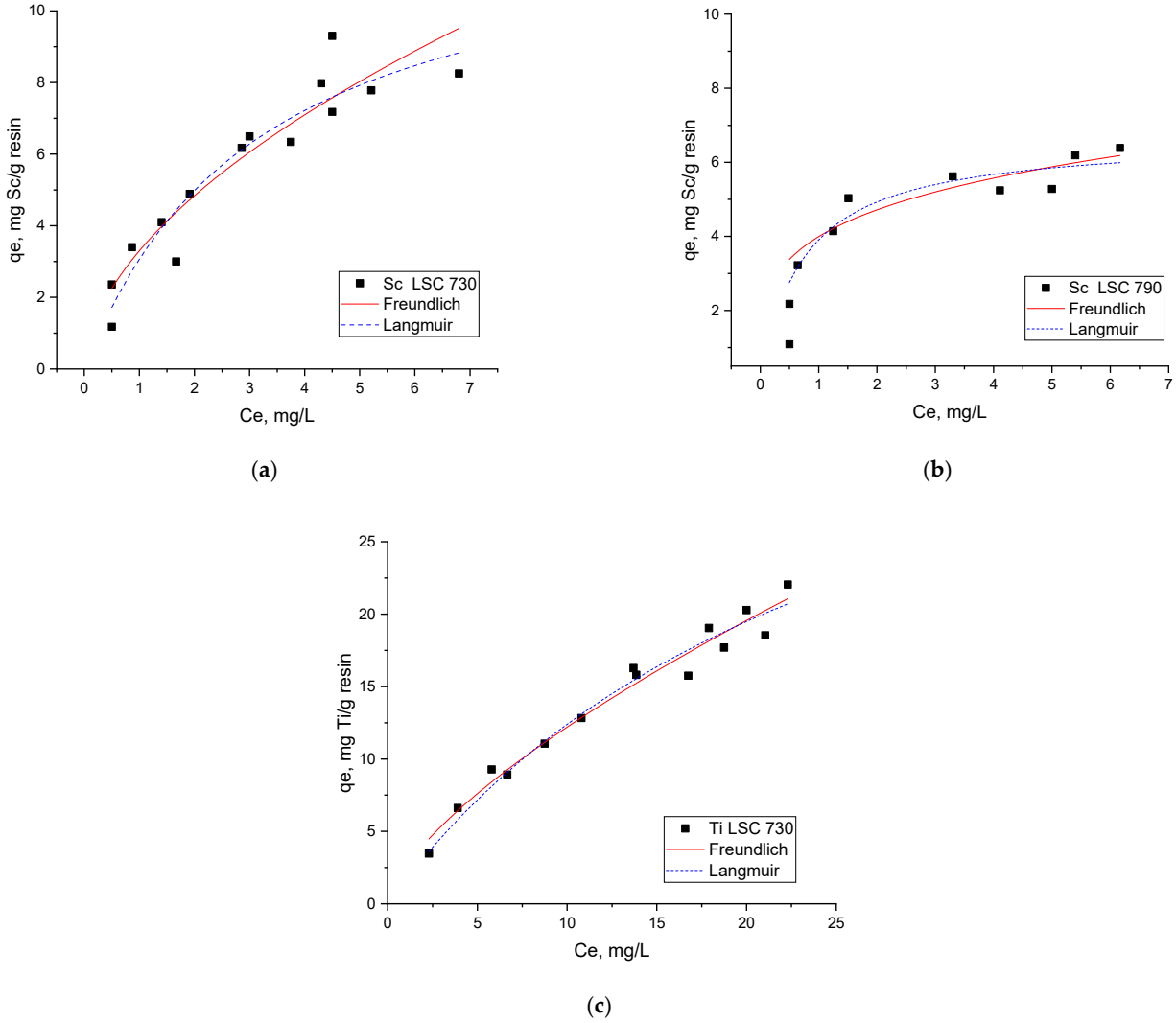

Figure 3. Freundlich and Langmuir adsorption isotherms for Sc (**a**,**b**) and Ti (**c**) adsorption for each resin.

Table 5. Correlation coefficients of experimental and calculated values, parameters of Freundlich and Langmuir models.

Resins	Metals	Freundlich Isotherm Constants			Langmuir Isotherm Constants		
		K_f	1/n	R^2	K_L	q_m	R^2
LSC 730	Sc	3.2992	0.5525	0.9776	0.3141	12.8056	0.9061
	Ti	2.540	0.6814	0.9920	0.0373	45.6269	0.9701
LSC 790	Sc	3.9935	0.2404	0.9843	1.4048	6.6827	0.9876

The Freundlich isotherm model is a more general expression than the Langmuir isotherm model. The Langmuir model is based on the assumption of monolayer adsorption and uses the constant q_m to represent the maximum adsorption capacity of the adsorbent. On the other hand, the Freundlich model is more suitable for describing cases of multilayer adsorption, but its parameter K_F does not have a clear physical interpretation [36]. As shown in Figure 3, the experimental results for the LSC 730 resin were found to be in good agreement with the Freundlich isotherm model for both Sc and Ti, suggesting that the adsorption of metals onto this resin material is heterogeneous and that the surface of the adsorbent has varying adsorption energies. According to Vigdorowitsch et al., 2021, the

amount of metal adsorbed per unit weight of adsorbent is not directly proportional to the concentration of the solute in the solution, and the adsorption intensity is observed to decrease with increasing solute concentrations [49]. For the LSC 790 resin, the Langmuir and the Freundlich models fit the experimental data well, with R^2 values of 0.9876 and 0.9843, respectively. Therefore, it is not concluded from the results of the adsorption isotherms if the adsorption sites are equivalent or not equivalent energetically [50].

3.2. Investigation of Feed Solution—Optimum Pretreatment

3.2.1. Preliminary Experiments

Experiments with four different pregnant liquor solution adjustments were performed to identify the optimal conditions for each resin: (i) no pretreatment, (ii) only acidification, (iii) only iron reduction, and (iv) both iron reduction and acidification exceeding a range of pH values from 0.19 to 3.6. The results are presented in Figure 4.

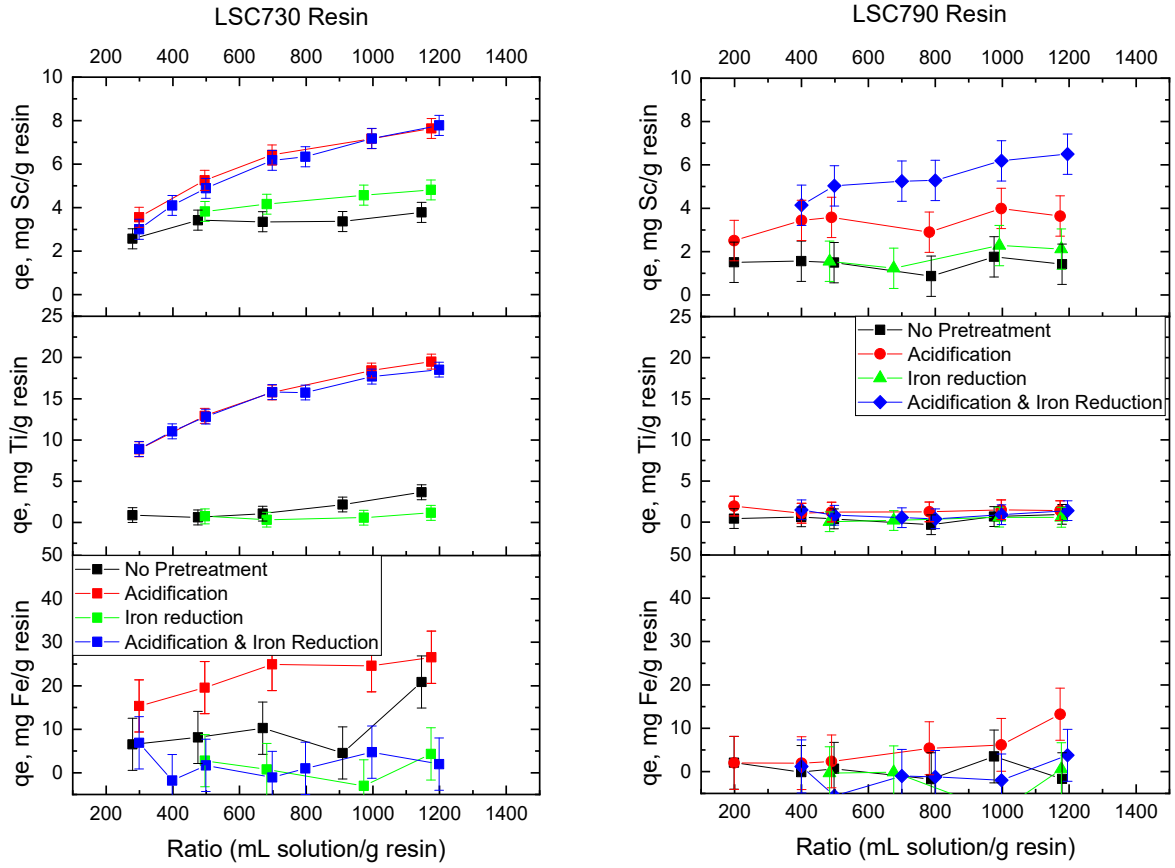

Figure 4. Preliminary experiments with four different solution adjustments: (i) no pretreatment, (ii) acidification, (iii) iron reduction, and (iv) iron reduction and acidification for LSC 730 (**a**) and LSC 790 resins (**b**).

The findings in Figure 4 suggest that without any pre-treatment of the solution and with only adding elemental iron for the iron reduction, the Sc adsorption for both resins was substantially decreased, along with impurities, such as titanium and iron.

In the case of the LSC 730 resin (Figure 4a), acidification of the solution resulted in a significant increase in the adsorption of scandium, as well as titanium and iron. However, when acidification was accompanied by iron reduction, a high level of scandium and titanium adsorption was achieved without any iron adsorption in the resin. It is observed in Figure 4a that the results of Sc adsorption from an acidified solution with and without Fe

(III) reduction are identical, suggesting that in the LSC 730 resin, there was no competitive interaction between the Fe and Sc ions.

Regarding the LSC 790 resin (Figure 4b), it was observed that neither iron nor titanium adsorption occurred under any condition tested. However, the combination of acidification and iron reduction led to the highest efficiency in terms of scandium adsorption. In summary, the incorporation of elemental iron was found to be a crucial factor in the overall effectiveness of the adsorption process. As depicted in Figure 4b, the adsorption of scandium was reduced in the acidified solution containing Fe (III) ions in comparison to the acidified solution containing Fe (II) ions. Furthermore, there was an increase in iron adsorption from the acidified solution containing Fe (III) ions, indicating the presence of a competitive interaction between the Fe (III) and Sc ions.

3.2.2. Adjustment of pH of Feed Solution

Follow-up experiments were carried out to investigate the impact of the pH on the adsorption characteristics of scandium, titanium, and iron. This was achieved by varying the concentration of H_2SO_4 added, with a standard addition of metallic Fe, which resulted in pH values ranging from 0.5 to 3.6. The exploration of higher pH values was limited due to the precipitation of ferric iron and scandium [51,52]. The study employed two different L/S ratios, namely 500:1 and 1000:1 mL of solution per gram of resin to further explore the adsorption behavior of the metals. In Figure 5, the efficiencies of Fe, Ti, and Sc are presented according to different pH values.

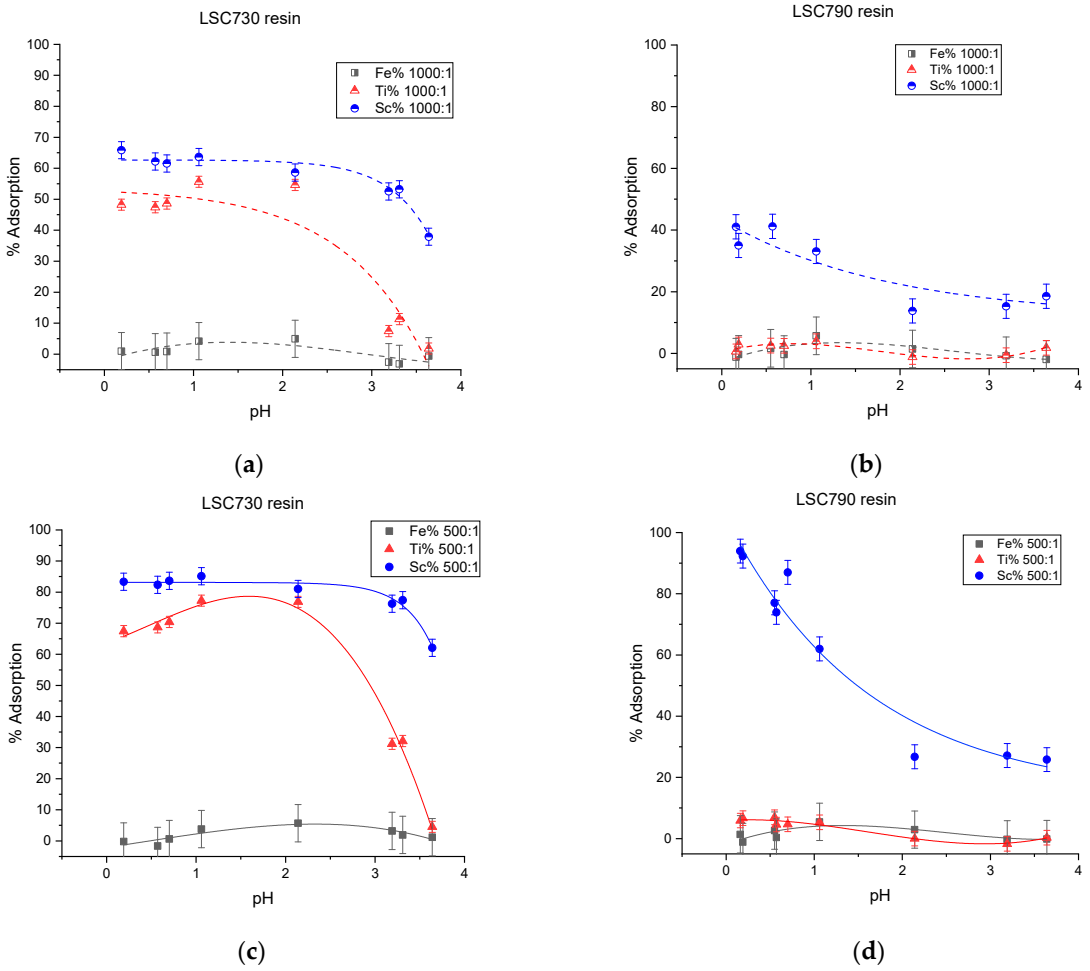

Figure 5. Impact of pH on the adsorption characteristics of scandium, titanium, and iron for LSC 730 at ratios of 1000:1 mL of solution per g of resin (**a**) and 500:1 mL/g (**c**) and for LSC 790 (**b**,**d**), respectively.

According to the results, the LSC 730 resin at the 1000:1 L/S ratio exhibited an adsorption capacity of approximately 19% less for scandium when the pH was maintained at around 3.2, while the adsorption capacity for Ti was approximately 77% less, thus making this pH favorable for achieving higher Sc selectivity towards Ti. The LSC 790 resin demonstrated the highest scandium adsorption at a pH level lower than 0.7, with almost negligible adsorption of both the Ti and Fe ions.

Based on the observations presented in Figure 5, the optimal solution for conducting kinetic experiments was selected for each resin by identifying the solution that exhibited the highest Sc adsorption efficiency and minimal impurities. Table 6 summarizes the optimal conditions for each resin.

Table 6. Conditions resulting in the highest degree of adsorption efficiency/selectivity. Values are given per liter of initial PLS.

Resin Tested	Fe (0) g/L	18M H_2SO_4 mL/L	pH of Solution
LSC 790	0.3	17	0.6
LSC730	0.3	1.6	3.2

3.3. Investigation of Sc Adsorption Kinetics by Batch Experiments

Kinetic experiments were performed for each resin using the optimum pretreated solution, as shown in Table 5. The effect of the liquid-to-solid ratio was studied by conducting batch tests at three different L/S ratios (250:1, 500:1, 1000:1). The kinetic results are shown in Figure 6.

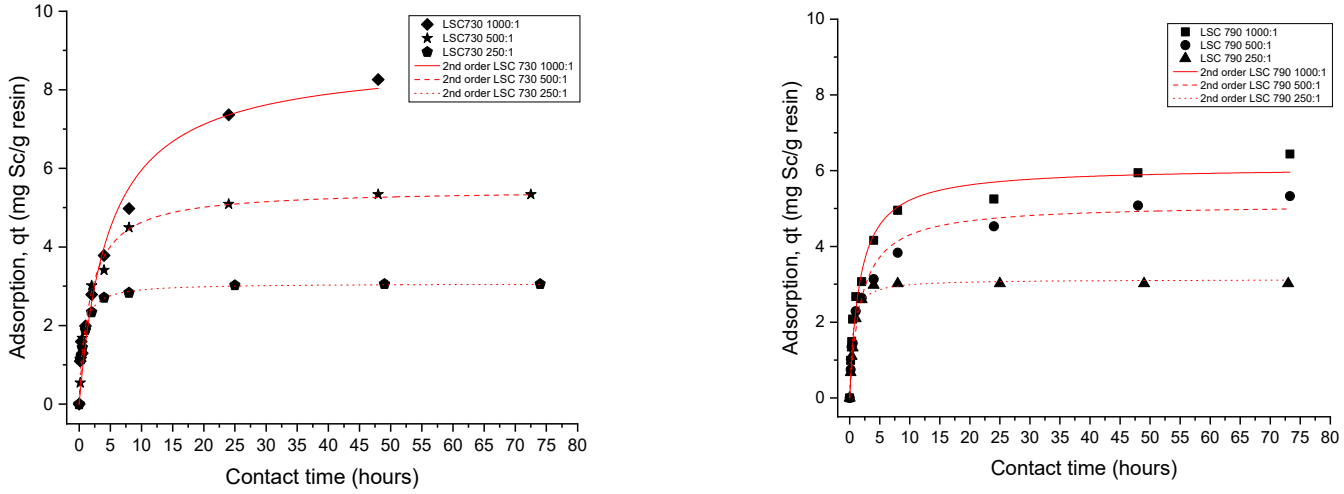

(**a**) (**b**)

Figure 6. Effect of L/S ratio on adsorption kinetics with (**a**) LSC 730 and (**b**) LSC 790 resins.

The kinetic data indicate that the Sc adsorption on both resins followed pseudo-second-order kinetics, and the rate constants (k), as well as the equilibrium concentration of Sc (qe), are shown in Table 7. The observed correlation, where higher solution volumes corresponded to slower scandium sorption onto the resin, can be attributed to the reduced interaction between the resin and target metal ions as the solution volume increased. The correlation coefficient R^2 resulting from the least square linear regression ranged from 0.9996 to 1. The results show that the Sc adsorption kinetics on both the LSC 730 and LSC 790 resins was low. The results of Table 7 show that the kinetics of adsorption on LSC 790 resin was faster than on LSC 730, as the relevant rate constants were higher in the case of LSC 790 resin.

Table 7. Comparison of adsorption rate constants; experimental and calculated q_e values for the pseudo-first- and second-order reaction kinetics of removal of scandium by LSC 730 and LSC 790 resins.

			Pseudo-Second-Order		
Resin	**L/S Ratio (mL/g)**	**Initial Sc Concentration (mg/L)**	**k_2 (g/mg min)**	**$q_{e,calc.}$ (mg/g)**	**R^2**
LSC 730	1000:1	12.8	0.0233	8.8484	0.9996
LSC 730	500:1	12.8	0.1014	5.4619	1.0000
LSC 730	250:1	12.8	0.5733	3.0712	1.0000
LSC 790	1000:1	12.7	0.0980	6.0953	0.9999
LSC 790	500:1	12.8	0.1038	5.1159	1.0000
LSC 790	250:1	12.6	0.6790	3.1287	1.0000

The initial adsorption rates were very fast for both resins, as seen in Figure 6, but after 3–4 h, the process decelerated, reaching a pseudo-equilibrium state. At this state, the rate of Sc adsorption was too low and became faster as the L/S ratio increased, which was equivalent to the increase in the ratio of Sc ions in the solution available for adsorption to the adsorption sites on the resin. This resembled a mass-transferred control process, which became faster as the L/S ratio increased. In addition, the L/S ratio, in the case of both resins, affected the adsorption capacity of Sc at the pseudo-equilibrium state. For the LSC 730 resin at an L/S of 250:1, the Sc capacity was almost 3.07 mg/g (Table 7), which was almost 24% of the maximum Sc capacity of this resin (12.8 mg/g, Table 5), while at an L/S of 500:1, it was 42.6%, and at an L/S of 1000:1, it was 69%. For the LSC 790 resin, at an L/S of 250:1, the Sc capacity was almost 3.13 mg/g (Table 7), which was almost 46.8% of the maximum Sc capacity of this resin (6.68 mg/g, Table 5), while at an L/S of 500: 1, it was 42.6%, and at an L/S of 1000:1, it was 69%. For the LSC 790 resin, at an L/S of 250:1, the Sc capacity was almost 3.13 mg/g (Table 7), which was almost 46.8% of the maximum Sc capacity of this resin (6.68 mg/g, Table 5), while at an L/S of 500:1, it was 76.6%, and at an L/S of 1000:1, it was 91.2%. The LSC 790 resin performed kinetically better than the LSC 730 and reached very close to its saturation at high L/S ratios. The kinetic results indicate that both resins are heterogeneous in nature, with at least two different adsorption sites for Sc ions. Some are easily amenable to Sc ions for adsorption and represent the first steep part of the kinetic curves (very fast adsorption), while the others are almost inaccessible to Sc ions and represent the almost flat part of the kinetic curves (very slow adsorption). It seems that in the case of the LSC 790 resin, 45% of the adsorption sites were easily accessible to Sc, while in LSC 730, only 15% were amenable, and thus, LSC790 performed kinetically better than the LSC 730.

4. Conclusions

Based on the results, it is noted that resins containing iminodiacetic and sulfonic acid functional groups did not exhibit significant scandium (Sc) extraction, whereas those with phosphate functional groups showed comparatively better Sc extraction rates.

Seplite LSC 730 resin has been identified as an effective adsorbent for scandium. This resin adsorbs both Sc and Ti simultaneously, with the highest experimental adsorption capacity of Sc measured at approximately 8 mg Sc/g, and that of Ti at approximately 22 mg Ti/g, while the adsorption of Fe was relatively insignificant. The experimental results for the LSC 730 resin are consistent with the Freundlich isotherm adsorption model for both Sc and Ti, indicating that the adsorption of metals onto this resin is heterogeneous, with varying adsorption energies on its surface. Acidification of the solution resulted in a significant increase in the adsorption of scandium, titanium, and iron. However, when acidification was accompanied by iron reduction, a high level of scandium and titanium adsorption was achieved without any iron adsorption in the resin. At a pH of 3.2, the resin

had a higher selectivity of Sc towards Ti; by sacrificing approximately 19% of the scandium, 77% less Ti was adsorbed.

Seplite LSC 790 resin is highly selective for scandium and showed the highest adsorption capacity of approximately 6.5 mg Sc/g resin. Both the Langmuir and Freundlich models were used to fit the Sc adsorption experimental data, and they showed a good correlation, with R^2 values of 0.9876 and 0.9843, respectively. However, since the R^2 values are so close, it cannot be concluded from the adsorption isotherms whether the adsorption sites had equivalent or non-equivalent energetic properties. The resin demonstrated the highest scandium adsorption at a pH level lower than 0.7, with almost negligible adsorption of both Ti and Fe ions. Nevertheless, the highest efficiency in terms of scandium adsorption was achieved when the acidified Fe(II) PLS was used. The reduction of Fe(III) to Fe(II) was found to be a crucial factor in the overall effectiveness of the adsorption process since, if the reduction was not performed, the adsorption of Sc decreased substantially, while the iron adsorption experienced a high increase, indicating a competitive interaction between the Fe(III) and Sc ions.

The kinetic results suggest that both resins are heterogeneous, meaning that they have multiple sites available for the adsorption of Sc ions. Some of these sites are easily accessible for Sc ions, resulting in fast adsorption (less than 10 h), while others are almost inaccessible, leading to slow adsorption (up to 3 days). Based on these findings, it appears that LSC 790 had a higher proportion (45%) of easily accessible sites for Sc adsorption compared to LSC 730, which only had a 15% proportion of accessible sites. Therefore, LSC 790 performed better kinetically in terms of Sc adsorption compared to LSC 730.

In general, LSC 790 was found to be more selective for Sc towards Ti and Fe, while LSC 730 had a higher extraction capacity for Sc extraction. Both resins merit further research for their elution and recyclability potential.

Summarizing, it would be valuable to explore a wider range of experimental parameters to understand the effects of different variables on the adsorption process. Further research is needed to explore the elution efficiency and methods to regenerate the resins for repeated use. This includes investigating alternative elution agents or conditions that allow for the efficient recovery of Sc from the resin while maintaining the integrity of the resin. Additional research using fixed-bed column experiments is recommended to enhance the understanding and utilization and enable the evaluation of the regeneration and reusability of the resins, contributing to a more sustainable and economically viable approach.

Author Contributions: Conceptualization, A.T., E.M., A.T. and D.P.; methodology, A.T., E.M. and D.M.; validation, D.M., E.B. and D.P.; data curation A.T. and E.M.; writing—original draft preparation, A.T., E.M. and D.M.; writing—review and editing, E.B. and D.P.; supervision E.B. and D.P.; All authors have read and agreed to the published version of the manuscript.

Funding: This research was funded by EIT, SCALE-UP KIC Project (2022–2024), project number 21013.

Data Availability Statement: The data presented in this study are available on request from the corresponding author.

Conflicts of Interest: The authors declare no conflict of interest.

References

1. Sammes, N.; Smirnova, A.; Vasylyev, O. (Eds.) Fuel Cell Technologies: State and Perspectives. In Proceedings of the NATO Advanced Research Workshop, Kyiv, Ukraine, 6–10 June 2004; Springer Science & Business Media: Berlin/Heidelberg, Germany, 2005.
2. Royset, J. Scandium in Aluminium Alloys Overview: Physical Metallurgy, Properties and Applications. *Metall. Sci. Technol.* **2007**, *25*, 12–21.
3. Grohol, M.; Veeh, C. Study on the Critical Raw Materials for the EU 2023. In *Internal Market, Industry, Entrepreneurship and SMEs*; Final Report; European Commission: Brussels, Belgium, 2023.
4. Sawtell, R.R.; Jensen, C.L. Mechanical Properties and Microstructures of Al-Mg-Sc Alloys. *Met. Trans. A* **1990**, *21*, 421–430. [CrossRef]
5. Ahmad, Z. The Properties and Application of Scandium-Reinforced Aluminum. *JOM* **2003**, *55*, 35–39. [CrossRef]

6. Phoung, S.; Williams, E.; Gaustad, G.; Gupta, A. Exploring Global Supply and Demand of Scandium Oxide in 2030. *J. Clean. Prod.* **2023**, *401*, 136673. [CrossRef]
7. Petrakova, O.; Kozyrev, A.; Suss, A.; Panov, A.; Gorbachev, S.; Perestoronina, M.; Vishnyakov, S. Industrial Trials Results of Scandium Oxide Recovery from Red Mud at UC RUSAL Alumina Refineries. In Proceedings of the TRAVAUX 48, Proceedings of the 37thInternational ICSOBA Conference andXXV Conference «Aluminium of Siberia», Krasnoyarsk, Russia, 16–20 September 2019; Volume 48.
8. Junior, A.B.; Espinosa, D.; Vaughan, J.; Tenório, J. Recovery of Scandium from Various Sources: A Critical Review of the State of the Art and Future Prospects. *Miner. Eng.* **2021**, *172*, 107148. [CrossRef]
9. Wang, W.; Pranolo, Y.; Cheng, C.Y. Metallurgical Processes for Scandium Recovery from Various Resources: A Review. *Hydrometallurgy* **2011**, *108*, 100–108. [CrossRef]
10. Xiao, J.; Zou, K.; Zhong, N.; Gao, D. Selective Separation of Iron and Scandium from Bayer Sc-Bearing Red Mud. *J. Rare Earths* **2022**, *14*, 1099–1107. [CrossRef]
11. Kalashnikov, A.; Yakovenchuk, V.; Pakhomovsky, Y.; Bazai, A.; Sokharev, V.; Konopleva, N.; Mikhailova, J.; Goryainov, P.; Ivanyuk, G. Scandium of the Kovdor Baddeleyite–Apatite–Magnetite Deposit (Murmansk Region, Russia): Mineralogy, Spatial Distribution, and Potential Resource. *Ore Geol. Rev.* **2015**, *72*, 532–537. [CrossRef]
12. Seredkin, M.; Zabolotsky, A.; Jeffress, G. In Situ Recovery, an Alternative to Conventional Methods of Mining: Exploration, Resource Estimation, Environmental Issues, Project Evaluation and Economics. *Ore Geol. Rev.* **2016**, *79*, 500–514. [CrossRef]
13. Borra, C.R.; Pontikes, Y.; Binnemans, K.; Van Gerven, T. Leaching of Rare Earths from Bauxite Residue (Red Mud). *Miner. Eng.* **2015**, *76*, 20–27. [CrossRef]
14. Aung, W.M.; Marchenko, M.V.; Troshkina, I.D. Sorption of Scandium from Sulfuric–Chloride Solutions by Activated Carbons. *Russ. J. Non-Ferrous Met.* **2019**, *60*, 646–651. [CrossRef]
15. Pirozhenko, K.Y.; Sokolova, Y.V.; Teselkina, A.E.; Glinskaya, I.V. The Sorption Recovery of Scandium from Sulfuric Acid Solution by Spherically Granulated Titanium Phosphate. *Sorpt. Chromatogr. Process.* **2016**, *16*, 306–312.
16. Molchanova, T.V.; Akimova, I.D.; Tatarnikov, A.V. Ion-Exchange Methods of Scandium Recovery from the Ores of the Tomtor Deposit. *Russ. Met. (Metally)* **2019**, *2019*, 674–679. [CrossRef]
17. Medvedev, A.S.; Khayrullina, R.T.; Kirov, S.S.; Suss, A.G. Technical Scandium Oxide Obtaining from Red Mud of Urals Aluminium Smelter. *Tsvetnye Met.* **2015**, *12*, 47–52. [CrossRef]
18. Smyshlyaev, V.Y. By-Producing Scandium from Pregnant Solutions during in-Situ Leaching at Dalmatovskoe Uranium Deposit. *Gorn. Zhurnal* **2017**, *8*, 28–32. [CrossRef]
19. Senik, E.; Vinogradov, M.; Taranov, R.; Kozodaev, A.; Ksenofontov, B.; Ksyenofontov, B.; Voropaeva, A. Rare Earth Metals Leaching from Coal Ash and Theirs Concentration. *Saf. Technosphere* **2016**, *5*, 48–55. [CrossRef]
20. Shoppert, A.; Valeev, D.; Diallo, M.M.; Loginova, I.; Beavogui, M.C.; Rakhmonov, A.; Ovchenkov, Y.; Pankratov, D. High-Iron Bauxite Residue (Red Mud) Valorization Using Hydrochemical Conversion of Goethite to Magnetite. *Materials* **2022**, *15*, 8423. [CrossRef]
21. Klauber, C.; Gräfe, M.; Power, G. Bauxite Residue Issues: II. Options for Residue Utilization. *Hydrometallurgy* **2011**, *108*, 11–32. [CrossRef]
22. Kumar, S.; Kumar, R.; Bandopadhyay, A. Innovative Methodologies for the Utilisation of Wastes from Metallurgical and Allied Industries. *Resour. Conserv. Recycl.* **2006**, *48*, 301–314. [CrossRef]
23. Wen, Z.-C.; Ma, S.-H.; Zheng, S.-L.; Zhang, Y.; Liang, Y. Assessment of Environmental Risk for Red Mud Storage Facility in China: A Case Study in Shandong Province. *Environ. Sci. Pollut. Res.* **2016**, *23*, 11193–11208. [CrossRef]
24. Rai, S.; Bahadure, S.; Chaddha, M.; Agnihotri, A. Use of Red Mud as Advanced Soil Stabilization Material. In *Advanced Materials from Recycled Waste*; Elsevier: Amsterdam, The Netherlands, 2023; pp. 45–56. [CrossRef]
25. Liu, X.; Han, Y.; He, F.; Gao, P.; Yuan, S. Characteristic, Hazard and Iron Recovery Technology of Red Mud—A Critical Review. *J. Hazard. Mater.* **2021**, *420*, 126542. [CrossRef]
26. Qaidi, S.; Tayeh, B.A.; Isleem, H.F.; de Azevedo, A.R.; Ahme, H.U.; Emad, W. Sustainable Utilization of Red Mud Waste (Bauxite Residue) and Slag for the Production of Geopolymer Composites: A Review. *Case Stud. Constr. Mater.* **2022**, *16*, e00994. [CrossRef]
27. Ochsenkuehn-Petropoulou, M.; Tsakanika, L.-A.; Lymperopoulou, T.; Ochsenkuehn, K.-M.; Hatzilyberis, K.; Georgiou, P.; Stergiopoulos, C.; Serifi, O.; Tsopelas, F. Efficiency of Sulfuric Acid on Selective Scandium Leachability from Bauxite Residue. *Metals* **2018**, *8*, 915. [CrossRef]
28. Gentzmann, M.C.; Schraut, K.; Vogel, C.; Gäbler, H.-E.; Huthwelker, T.; Adam, C. Investigation of Scandium in Bauxite Residues of Different Origin. *Appl. Geochem.* **2021**, *126*, 104898. [CrossRef]
29. Davris, P.; Balomenos, E.; Nazari, G.; Abrenica, G.; Patkar, S.; Xu, W.-Q.; Karnachoritis, Y. Viable Scandium Extraction from Bauxite Residue at Pilot Scale. *Mater. Proc.* **2022**, *5*, 129. [CrossRef]
30. Hubicki, Z.; Kołodyńska, D. Selective Removal of Heavy Metal Ions from Waters and Waste Waters Using Ion Exchange Methods. *Environ. Sci.* **2012**, *7*, 193–240. [CrossRef]
31. Zhu, X.; Li, W.; Tang, S.; Zeng, M.; Bai, P.; Chen, L. Selective Recovery of Vanadium and Scandium by Ion Exchange with D201 and Solvent Extraction Using P507 from Hydrochloric Acid Leaching Solution of Red Mud. *Chemosphere* **2017**, *175*, 365–372. [CrossRef] [PubMed]

32. Mikeli, E.; Marinos, D.; Toli, A.; Pilichou, A.; Balomenos, E.; Panias, D. Use of Ion-Exchange Resins to Adsorb Scandium from Titanium Industry's Chloride Acidic Solution at Ambient Temperature. *Metals* **2022**, *12*, 864. [CrossRef]
33. Sharaf, M.; Yoshida, W.; Kubota, F.; Goto, M. A Novel Binary-Extractant-Impregnated Resin for Selective Recovery of Scandium. *J. Chem. Eng. Jpn.* **2019**, *52*, 49–55. [CrossRef]
34. Salman, A.D.; Juzsakova, T.; Mohsen, S.; Abdullah, T.A.; Le, P.-C.; Sebestyen, V.; Sluser, B.; Cretescu, I. Scandium Recovery Methods from Mining, Metallurgical Extractive Industries, and Industrial Wastes. *Materials* **2022**, *15*, 2376. [CrossRef]
35. Mikhaylenko, M. Development and Screening of Resins to Recover REE and Scandium from Different Sources. In *Extraction 2018: Proceedings of the First Global Conference on Extractive Metallurgy*; Springer International Publishing: Berlin/Heidelberg, Germany, 2018; pp. 2113–2122. [CrossRef]
36. Foo, K.; Hameed, B. Insights into the Modeling of Adsorption Isotherm Systems. *Chem. Eng. J.* **2010**, *156*, 2–10. [CrossRef]
37. Balomenos, E.; Davris, P.; Apostolopoulou, A.; Marinos, D.; Mikeli, E.; Toli, A.; Kotsanis, D.; Paschalis, G.; Panias, D. Investigations into Optimized Industrial Pilot Scale BR Leaching for Sc Extraction. In *TMS Annual Meeting & Exhibition*; Springer Nature Switzerland: Cham, Switzerland, 2023; pp. 1167–1172. [CrossRef]
38. Mostajeran, M.; Bondy, J.-M.; Reynier, N.; Cameron, R. Mining Value from Waste: Scandium and Rare Earth Elements Selective Recovery from Coal Fly Ash Leach Solutions. *Miner. Eng.* **2021**, *173*, 107091. [CrossRef]
39. Altinsel, Y.; Topkaya, Y.; Kaya, Ş.; Şentürk, B. Extraction of Scandium from Lateritic Nickel-Cobalt Ore Leach Solution by Ion Exchange: A Special Study and Literature Review on Previous Works. In *TMS 2018: Light Metals 2018*; Minerals, Metals and Materials Series; Springer International Publishing: Berlin/Heidelberg, Germany, 2018; Volume Part F4, pp. 1545–1553. [CrossRef]
40. Alkan, G.; Schier, C.; Gronen, L.; Stopic, S.; Friedrich, B. A Mineralogical Assessment on Residues after Acidic Leaching of Bauxite Residue (Red Mud) for Titanium Recovery. *Metals* **2017**, *7*, 458. [CrossRef]
41. Wood, S.A.; Samson, I.M. The Aqueous Geochemistry of Gallium, Germanium, Indium and Scandium. *Ore Geol. Rev.* **2006**, *28*, 57–102. [CrossRef]
42. Bao, S.; Hawker, W.; Vaughan, J. Scandium Loading on Chelating and Solvent Impregnated Resin from Sulfate Solution. *Solvent Extr. Ion Exch.* **2018**, *36*, 100–113. [CrossRef]
43. Tan, K.; Hameed, B. Insight into the Adsorption Kinetics Models for the Removal of Contaminants from Aqueous Solutions. *J. Taiwan Inst. Chem. Eng.* **2017**, *74*, 25–48. [CrossRef]
44. Smirnov, A.L.; Titova, S.M.; Rychkov, V.N.; Bunkov, G.M.; Semenishchev, V.S.; Kirillov, E.V.; Poponin, N.N.; Svirsky, I.A. Study of Scandium and Thorium Sorption from Uranium Leach Liquors. *J. Radioanal. Nucl. Chem.* **2017**, *312*, 277–283. [CrossRef]
45. Kilian, K.; Pyrzyńska, K.; Pęgier, M. Comparative Study of Sc(III) Sorption onto Carbon-Based Materials. *Solvent Extr. Ion Exch.* **2017**, *35*, 450–459. [CrossRef]
46. Yessimkanova, U.; Mataev, M.; Alekhina, M.; Kopbaeva, M.; Berezovskiy, A.; Dreisinger, D. The Study of the Kinetic Characteristics of Sorption of Scandium of Ion Exchanger Purolite Mts9580 from Return Circulating Solutions of Underground Leaching of Uranium Ores. *Eurasian Chem. J.* **2020**, *22*, 135–140. [CrossRef]
47. Adonis, S.; Oosthuysen, T. Evaluation of Scandium Sorption Using Modified Amberlite XAD-4 Resin. *Mon. Für Chem.-Chem. Mon.* **2022**, *153*, 1185–1196. [CrossRef]
48. Smyshlyaev, D.; Kirillov, E.; Kirillov, S.; Bunkov, G.; Rychkov, V.; Botalov, M.; Taukin, A.; Yuldashbaeva, A.; Malyshev, A. Recovery and Separation of Sc, Zr and Ti from Acidic Sulfate Solutions for High Purity Scandium Oxide Production: Laboratory and Pilot Study. *Hydrometallurgy* **2022**, *211*, 105889. [CrossRef]
49. Vigdorowitsch, M.; Pchelintsev, A.; Tsygankova, L.; Tanygina, E. Freundlich Isotherm: An Adsorption Model Complete Framework. *Appl. Sci.* **2021**, *11*, 8078. [CrossRef]
50. Ghodbane, I.; Hamdaoui, O. Removal of Mercury(II) from Aqueous Media Using Eucalyptus Bark: Kinetic and Equilibrium Studies. *J. Hazard. Mater.* **2008**, *160*, 301–309. [CrossRef] [PubMed]
51. Yagmurlu, B.; Dittrich, C.; Friedrich, B. Precipitation Trends of Scandium in Synthetic Red Mud Solutions with Different Precipitation Agents. *J. Sustain. Met.* **2017**, *3*, 90–98. [CrossRef]
52. Chernyaev, A.; Wilson, B.P.; Lundström, M. Study on Valuable Metal Incorporation in the Fe–Al Precipitate during Neutralization of LIB Leach Solution. *Sci. Rep.* **2021**, *11*, 23283. [CrossRef]